DOI: http://dx.doi.org/10.22104/ijhfc.2015.265

Iranian Journal of Hydrogen & Fuel Cell 4(2015) 227-240

Iranian Journal of Hydrogen & Fuel Cell

IJHFC

Journal homepage://ijhfc.irost.ir

Effect of sorbitol/oxidizer ratio on microwave assisted solution combustion synthesis of copper based nanocatalyst for fuel cell grade hydrogen production

Hossein Ajamein[1,2], Mohammad Haghighi[1,2,*]

[1] Chemical Engineering Faculty, Sahand University of Technology, P.O.Box 51335-1996, Sahand New Town, Tabriz, Iran.
[2] Reactor and Catalysis Research Center (RCRC), Sahand University of Technology, P.O.Box 51335-1996, Sahand New Town, Tabriz, Iran

Article Information

Article History:

Received:
02 February 2016
Received in revised form:
18 March 2016
Accepted:
10 April 2016

Keywords

$CuO-ZnO-Al_2O_3$
Microwave Combustion
Fuel/Oxidizer Ratio
Methanol Steam Reforming
Hydrogen.

Abstract

Steam reforming of methanol is one of the promising processes for on-board hydrogen production used in fuel cell applications. Due to the time and energy consuming issues associated with conventional synthesis methods, in this paper a quick, facile, and effective microwave-assisted solution combustion method was applied for fabrication of copper-based nanocatalysts to convert methanol to hydrogen. For this purpose, a series of nanocatalysts with different sorbitol/nitrates ratios were synthesized by the microwave-assisted combustion method. Their physicochemical properties were studied by XRD, FESEM, EDX, BET and FTIR analyses. It was found that enhancement of the sorbitol/nitrates ratio led to an increase of CuO dispersion and specific surface area, as well as smaller, nanometric and homogeneously dispersed particles. These significant characteristic properties, especially achieved by the CZA(S/N=3) nanocatalyst, resulted in high methanol conversion and hydrogen selectivity even at low temperatures. This effective performance was accompanied by negligible CO production as an undesired by-product as well as poison in fuel cell applications.

1. Introduction

Nowadays, fuel cell technology has become a promising alternative for conventional internal combustion engines. The fast growth of fuel cell applications depends on their interesting advantages such as low environmental impact, feed flexibility, silently operation and high efficiency [1, 2]. Hydrogen is the main feed of fuel cell systems, but it comes with some safety issues associated with utilization of this technology for vehicles. So, considering that hydrogen cannot be stored in the car's tank, the best solution may be on-board hydrogen production [3]. Several studies have focused on proposing a suitable fuel, including methanol, ethanol, dimethyl ether, and etc., for production of on-board hydrogen. Among

*Corresponding Author's Tel: +98-41-33458096 & +98-41-33459152, Fax: +98-41-33444355
E-mail address: haghighi@sut.ac.ir, http://rcrc.sut.ac.ir

them, methanol has attracted the most attention due to its interesting benefits [4-9]. High H/C ratio, lower sulfur content, no C-C bond and commercially large scale production from different sources can be counted as some of methanol main advantages [10]. Methanol can be converted to hydrogen through four pathways, namely methanol decomposition (MD), partial oxidation of methanol (POM), steam reforming of methanol (SRM) and auto thermal reforming of methanol (ATRM). Among these, steam reforming of methanol has good potential for production of on-board hydrogen at low temperatures with low CO content [11]. SRM can be demonstrated by the following main reactions:

$$CH_3OH + H_2O \rightarrow 3H_2 + CO_2 \quad \Delta H^{\circ}_{298} = 49.7(kJ/mol) \quad \text{(R1)}$$

$$CH_3OH \rightarrow CO + 2H_2 \quad \Delta H^{\circ}_{298} = 90.7(kJ/mol) \quad \text{(R2)}$$

$$CO_2 + H_2 \rightarrow CO + H_2O \quad \Delta H^{\circ}_{298} = 41.2(kJ/mol) \quad \text{(R3)}$$

The first reaction is the SRM reaction for production of hydrogen. Other side reactions, such as methanol decomposition (R2) and reverse water gas shift reaction (R3,) can occur during the SRM process as the main routes of CO production. Carbon monoxide is the undesired product of SRM, and is known as the poison for anodic catalyst of the fuel cells. Copper based catalysts are the most investigated catalysts for the SRM process because of their high conversion and hydrogen selectivity [12-15].

Many different synthesis methods have been studied for fabrication of copper based catalysts. The most common ones are co-precipitation and impregnation techniques [11, 16, 17]. However, these methods have very time and energy consuming steps including filtration, washing, drying and calcination [18]. One of the interesting and novel techniques for preparation of nanocatalysts is the solution combustion synthesis method (SCS). In contrast, this method is simple, rapid andis more energy saving [19, 20]. SCS is, in fact, an exothermically redox reaction between an organic fuel and an oxidizer agent (nitrate ions) which produces a huge volume of combustion gases. Different parameters such as fuel type, fuel/oxidizer ratio, atmosphere and pH can affect the quality of the resulting catalysts [21-23]. Various fuels, such as urea, glycine, oxalyldihydrazide, carbohydrazide, ethylene glycol and citric acid, have been suggested for SCS [24, 25].

Sorbitol ($C_6H_{14}O_6$) is a sugar alcohol mostly made from corn syrup with various medical applications. The reduction property of sorbitol as well as its hydrocarbon structure nominates it as a suitable fuel candidate for the SCS method. However, fewer studies have been performed on its influence for preparation of nanocatalysts by solution combustion method [26-30]. Therefore in this paper, the effect of sorbitol as the fuel for fabrication of CuO-ZnO-Al_2O_3 (CZA) nanocatalysts via the solution combustion method was investigated. Furthermore, to decrease synthesis time a microwave oven was used instead of a conventional furnace for preparation of the nanocatalysts. In addition, the influence of the sorbitol/nitrates ratio on the physicochemical characteristic and catalytic properties of the prepared nanocatalysts was studied. For this purpose, a series of CZA nanocatalysts were synthesized by the SCS method. Their physicochemical properties were analyzed by XRD, FESEM, EDX, BET and FTIR techniques. The catalytic performance of these nanocatalysts was tested in a laboratory catalytic apparatus designed for SRM reaction.

2. Materials and methods

2.1. Materials

Copper nitrate trihydrate ($Cu(NO_3)_2.3H_2O$, Merck, extra pure), zinc nitrate hexahydrate ($Zn(NO_3)_2.6H_2O$, Merck, extra pure), aluminium nitrate nonahydrate ($Al(NO_3)_3.9H_2O$, Merck, extra pure) and sorbitol (C6H14O6, Merck) were used as the nitrate precursors and the fuel for the solution combustion synthesis method. All the materials were used with no further purification.

2.2. Nanocatalysts preparation and procedure

As can be seen in Figure 1, the synthesis methodology can be divided into three sections: precursor preparation, combustion synthesis, and catalyst forming. Furthermore, Figure 2 depicts the synthesis of CuO-ZnO-Al_2O_3 catalysts by the microwave-assisted solution combustion method. At first, an aqueous solution of nitrate precursors with the proper molar ratio was prepared. The sorbitol powder was added to the nitrate solution and was mixed for 45 minutes. In the combustion synthesis section, the resulting mixture was heated at 80˚C to evaporate the excess water and to form a black blue viscous gel. Then, the gel was put in a microwave oven where it started to boil and smoke and finally ignited suddenly in less than 3 minutes. The synthesized catalysts were foamy and porous due to the huge amount of gases released during the combustion synthesis. The prepared catalysts were finally shaped to be easily loaded in the reactor.

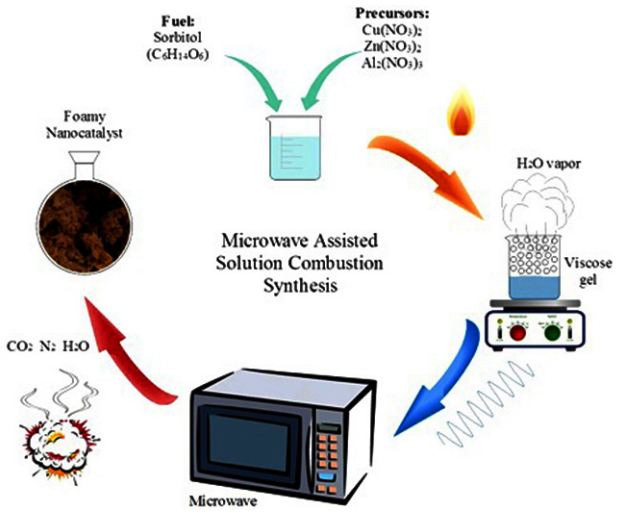

Fig. 2. Schematic stages for microwave assisted solution combustion synthesis of copper based nanocatalyst.

2.3. Nanocatalysts characterization techniques

The synthesized nanocatalysts were characterized by various analyses to discover their physicochemical

Fig. 1. Preparation steps of a copper based nanocatalyst via microwave assisted solution combustion synthesis.

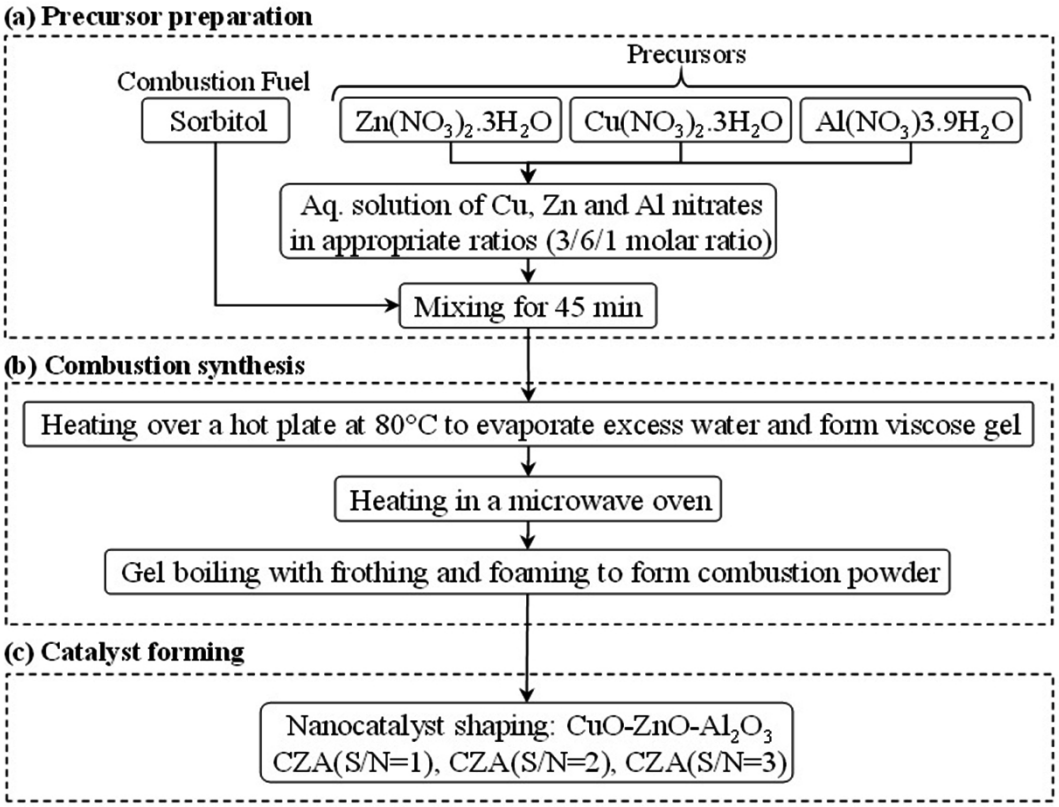

properties. X-ray diffraction analysis were applied to study the crystalline structure of the prepared nanocatalysts by a D-5000 Siemens diffractometer using Cu Kα radiation coupled to an X-ray tube works at 30 kV and 40 mA. The crystallite size of samples was calculated from XRD patterns by the Scherrer equation [31]. The morphology of the fabricated samples was investigated by Field Emission Scanning Electron Microscopy (FESEM) on a HITACHI S-4160 analyzer. A Quantachrome ChemBET 3000 analyser using N_2 adsorption and Brunauer-Emmett-Teller (BET) equation was used to measure the specific surface area. An energy dispersive X-ray analyzer (VEGA II, TESCAN) was used to analyze the surface elemental existence and dispersion of nanocatalysts. The Fourier Transform Infrared Spectroscopy (FTIR, Unicam 4000) using KBr plate was applied to identify the functional groups of nanocatalysts.

2.4. Experimental setup for catalytic performance test

As schematically illustrated in Figure 3, the catalytic performance of synthesized nanocatalysts was evaluated in a laboratory experimental setup. This experimental system was designed and used for the steam methanol reforming process at atmospheric pressure. The feed containing methanol and water, with a constant methanol/water ratio of 1.5, was kept in a saturator. It was introduced to a fixed bed reactor by an argon stream with a constant flow rate controlled by a mass flow controller. The SRM reactor is U-shape (5mm i.d.) and loaded with 400 mg of shaped nanocatalysts (cylinders with a height of 5 mm and a diameter of 3 mm). The loaded reactor was placed in an electrical furnace to apply the required heat of the endothermic reforming reaction. The SRM reaction was carried out in a temperature range of 160-300ºC and steady state conditions. The gas hourly space velocity was set on 10000 $cm^3/g.h$. The feed and product compositions were analysed by a gas chromatograph (GC Chrom, Teif Gostar Faraz, Iran). This system was equipped with a PLOT-U column as well as TCD and FID detectors. The conversion and selectivity of products were calculated as follows:

$$X_{CH_3OH}\% = \frac{F_{CH_3OH_{in}} - F_{CH_3OH_{out}}}{F_{CH_3OH_{in}}} \times 100 \quad (1)$$

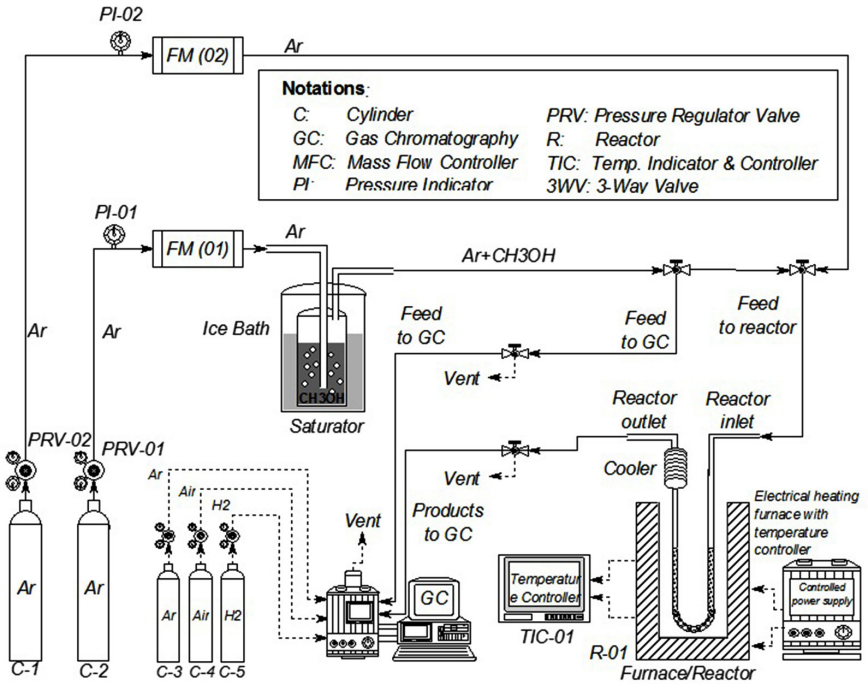

Fig. 3. Experimental setup for steam methanol reforming.

$$S_{H_2}\% = \frac{F_{H_{2out}}}{F_{H_{2out}} + F_{CO_{out}} + F_{CO_{2_{out}}}} \times 100 \quad (2)$$

$$S_{CO}\% = \frac{F_{CO_{out}}}{F_{H_{2out}} + F_{CO_{out}} + F_{CO_{2_{out}}}} \times 100 \quad (3)$$

$$S_{CO_2}\% = \frac{F_{CO_{2out}}}{F_{H_{2out}} + F_{CO_{out}} + F_{CO_{2_{out}}}} \times 100 \quad (4)$$

Where F_i is the molar flow rate of component *i* in the gaseous effluent.

3. Results and discussions

3.1. Nanocatalysts characterization

3.1.1. XRD analysis

The results of the crystallography analysis of prepared nanocatalysts are represented in Figure 4 and Table 1. The figure illustrates the XRD patterns of CuO-ZnO-Al_2O_3 nanocatalysts with different fuel/nitrate ratios at 2θ=20-90º. At first glance, the formation of a monoclinic phase of CuO and a hexagonal phase of ZnO can be clearly identified. Significant peaks of CuO (JCPDS 01-080-1268) were centered at 2θ= 35.5, 38.8, 48.8 and 68.2º [32]. Furthermore, peaks identified at 2θ=31.7, 34.4, 36.2, 47.5, 56.5 and 62.8º can be attributed to ZnO crystal (JCPDS 01-076-0704) [33]. No detectable peaks can be nominated for Al_2O_3 due to its amorphous phase and highly dispersed. It should be mentioned that, the enhancement of the sorbitol/oxidizer ratio resulted in a decrease of CuO and ZnO crystallinity. This phenomenon led to highly dispersed CuO and ZnO species in the prepared nanocatalysts. This was confirmed by the crystallite size results achieved by

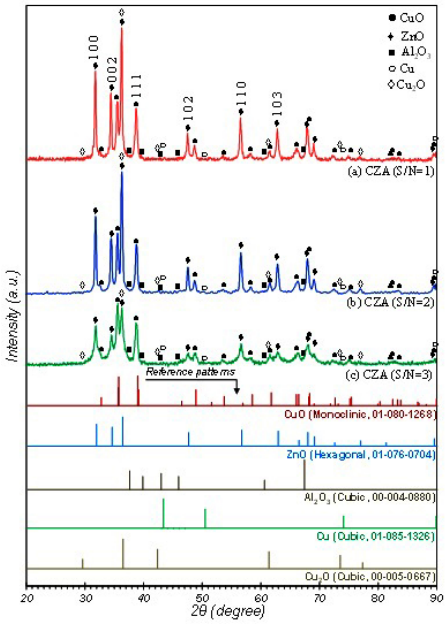

Fig. 4. XRD patterns of copper based nanocatalysts synthesized via the microwave assisted solution combustion method with various ratio of sorbitol/oxidizer: (a) CZA (S/N=1), (b) CZA (S/N=2) and (c) CZA (S/N=3).

the Scherrer equation and listed in Table 1. This table shows that an increase of the sorbitol/nitrate ratio caused a decrease in the CuO and ZnO crystallite size. However, this reduction was more sever for zinc oxide crystals. The relative crystallinity also approved the

Table 1. Specific surface area and crystallographic properties of synthesized copper based nanocatalysts.

Nanocatalyst	Sorbitol/Oxidizer (molar)	BET (m^2/g)	Relative Crystallinity[a]			Crystallite size[b] (nm)		
			CuO	ZnO	Al_2O_3	CuO[c]	ZnO[d]	Al_2O_3[e]
CZA (S/N=1)	1	33.1	100	100	-	23.4	31	-
CZA (S/N=2)	2	37.2	92.9	89.7	-	23.3	31.8	-
CZA (S/N=3)	3	63.4	75.7	44.8	-	17.4	19.9	-

a. Relative crystallinity: XRD relative peak intensity.
b. Crystallite size estimated by Scherre's equation.
c. Crystallite phase: monoclinic (JCPDS: 01-080-1268, 2θ = 35.5, 35.6, 38.8, 38.9, 48.8, 61.6, 68.2)
d. Crystallite phase: hexagonal (JCPDS: 01-076-0704, 2θ = 31.7, 34.4, 36.2, 47.5, 56.5, 62.8, 67.9, 69.0)
e. Crystallite phase: cubic (JCPDS: 00-004-0880, 2θ = 37.4, 39.7, 42.8, 45.8, 67.3)

decrease in crystallinity of the CuO and ZnO species. Therefore, as expected from the formed CuO crystals, CZA(S/N=3) might show higher catalytic activity in the steam methanol reforming reaction.

3.1.2. FESEM analysis

Figure 5 illustrates the surface morphology of the prepared nanocatalysts. The nanometric particles of the synthesized nanocatalysts can be proved by FESEM images. Moreover, enhancement of the sorbitol/oxidizer ratio led to smaller particles which might facilitate the accessibility of reactants to active sites. The homogeneity of particles increased by increasing as the fuel/nitrates ratio increased due to less agglomerates being formed. According to FESEM images, it can be supposed that the CZA(S/N=3), with highly homogeneous and small particles, might show higher activity than other samples in the steam methanol reforming process. To statistically represent the particle size distribution of the CZA(S/N=3) nanocatalyst, its surface particle size distribution histogram was calculated by ImageJ software [34] and is depicted in Figure 6. The narrow size distribution of the CZA(S/N=3) sample between 10-60 nm can be identified in this figure. The average surface particle size is about 24.6 nm which proves the nanometer structure of the synthesized catalyst.

3.1.3. EDX analysis

The EDX dot-mapping results of the fabricated

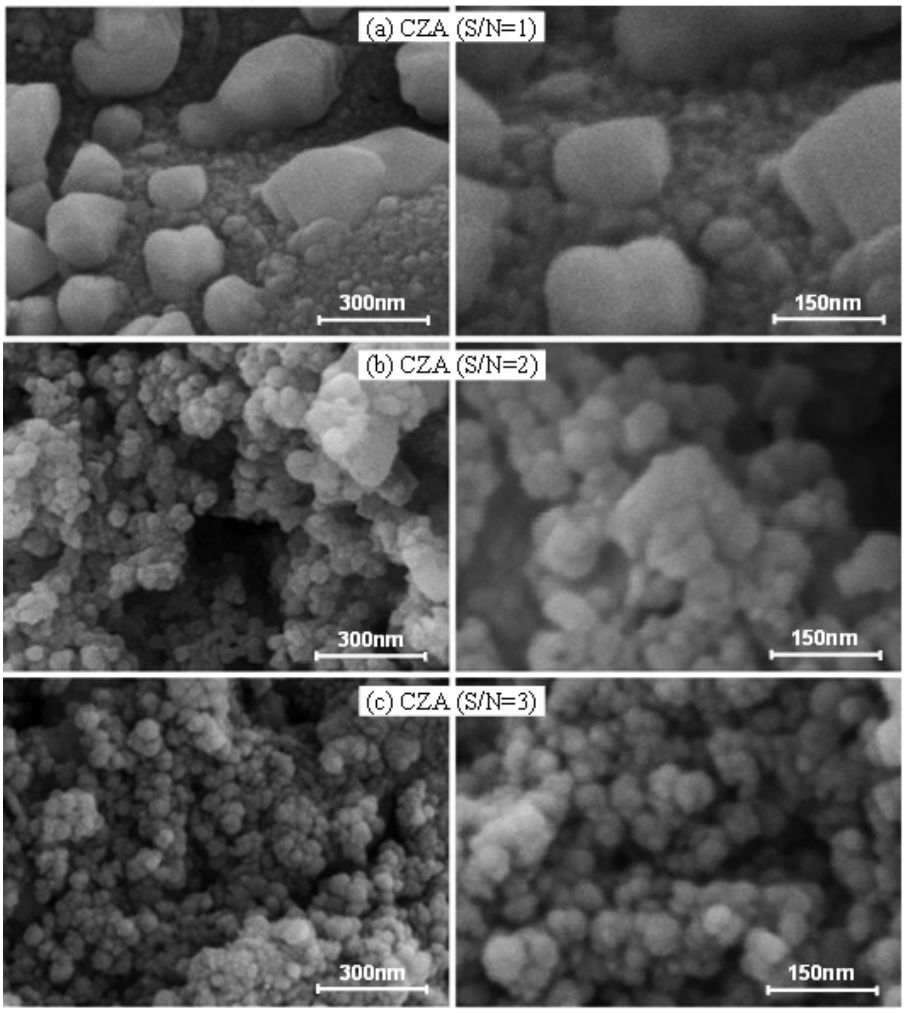

Fig. 5. FESEM images of copper based nanocatalysts synthesized via the microwave assisted solution combustion method with various ratio of sorbitol/oxidizer: (a) CZA (S/N=1), (b) CZA (S/N=2) and (c) CZA (S/N=3).

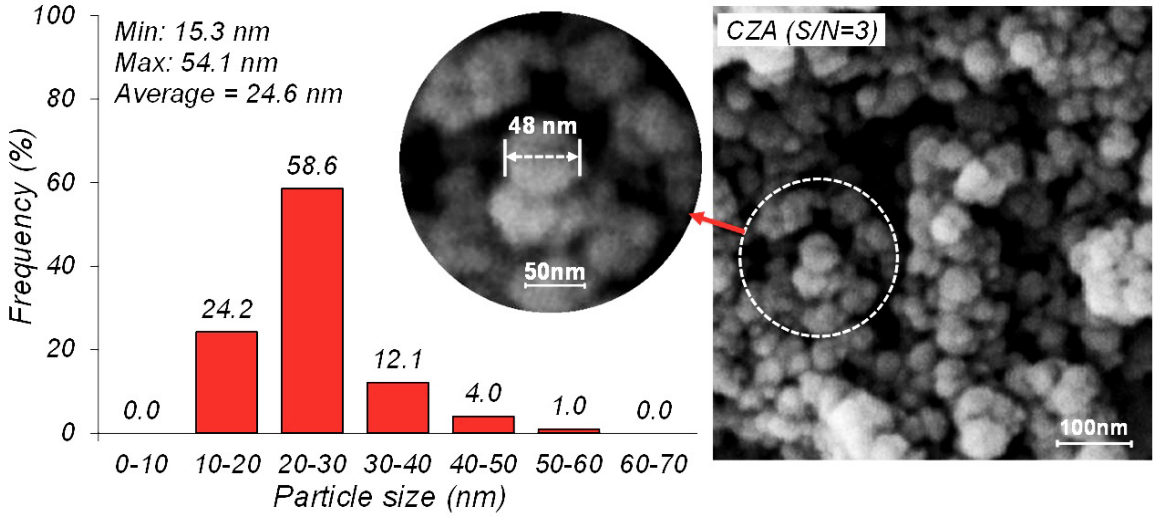

Figure 6. Surface particle size distribution histogram of the copper based nanocatalyst synthesized via the microwave assisted solution combustion method with a sorbitol/oxidizer ratio of 3: CZA (S/N=3).

nanocatalysts with different fuel/nitrates ratios are depicted in Figure 7. The presence of all elements used in the preparation of nanocatalysts, especially aluminium which was not identified from other analyses, was the main result obtained from the EDX spectra. Moreover, the surface composition of the final nanocatalysts and their primary gel was similar which proved no material loss during the synthesis route occurred. As can be seen from the EDX spectra, dispersion of Cu and Zn species was well performed in the CZA(S/N=3) nanocatalyst. Therefore, the EDX results helped to predict that the CZA(S/N=3) might show higher catalytic performance due to its suitable characterization.

3.1.4. BET analysis

The catalytic performance of the nanocatalyst as a surface adsorption mechanism is highly dependent on specific surface area. In this paper, the specific surface area of the fabricated nanocatalysts was calculated by the Brunauer–Emmett–Teller analysis (BET) as listed in Table 1. Increase in the sorbitol/nitrates ratio led to enhancement of the surface area especially for the CZA(S/N=2) and CZA(S/N=3) nanocatalysts.

A comparison of these nanocatalysts showed that the specific surface area of the CZA(S/N=3) nanocatalyst is about 41% higher than the CZA(S/N=2) sample. So, we expected that the CZA(S/N=3) nanocatalyst would shows higher catalytic activity than CZA(S/N=1) and CZA(S/N=2) nanocatalysts.

3.1.5. FTIR analysis

The FTIR spectra illustrated in Figure 8 address the functional groups of synthesized nanocatalysts. Observation of the spectra reveals that all the samples have nearly similar significant peaks due to their same functional groups. From the literature we know metal oxides lead to stretching frequencies in the range of 430-700 cm^{-1} [35]. More precisely, the bands at 430 and 495 cm^{-1} can be assigned to Cu-O and Zn-O species, respectively [36]. Also, Al-O stretching vibration can be identified by the peak near 700 cm^{-1} [37]. The inter layer water molecules [38-40] and hydroxide group [41-43] might be left over from the synthesis steps exhibited in bands at 1580 and 3450 cm^{-1}, respectively. Sorbitol consists of hydrogen and carbon atoms which can produce carbon dioxide during its reaction with nitrates or thermally decomposition. Therefore,finding carbonated species formed by adsorbed CO_2 on the nanocatalysts surface appearing at 1390 cm^{-1} was expected [44-46].

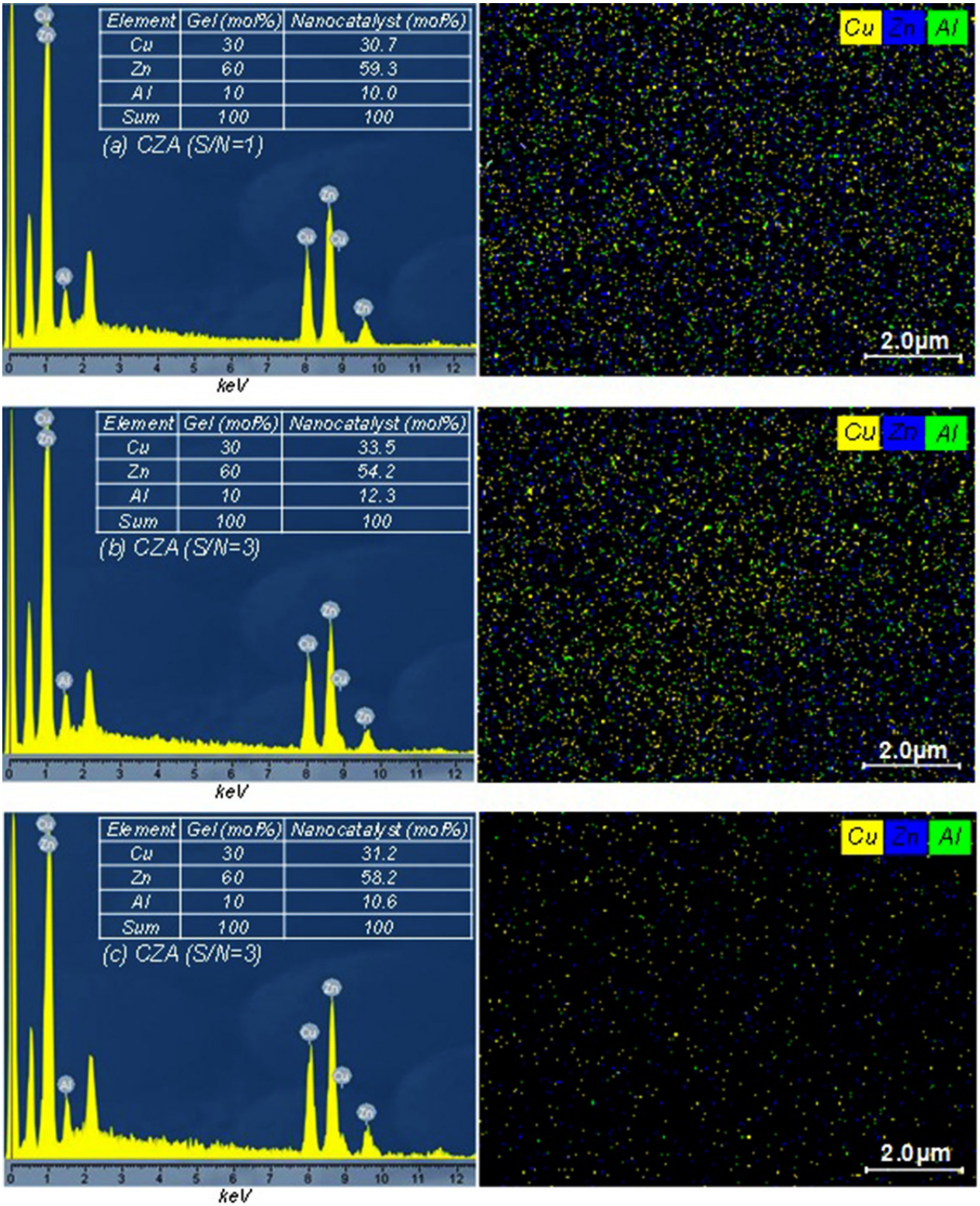

Fig. 7. EDX analysis of copper based nanocatalysts synthesized via the microwave assisted solution combustion method with various ratio of sorbitol/oxidizer: (a) CZA (S/N=1), (b) CZA (S/N=2) and (c) CZA (S/N=3).

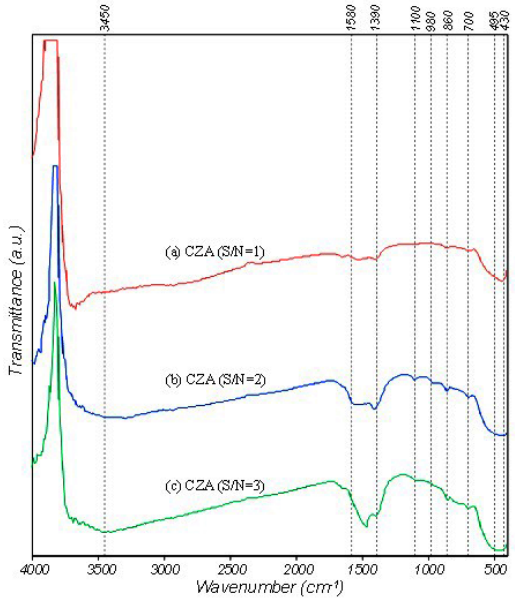

Fig. 8. FTIR spectra of copper based nanocatalysts synthesized via the microwave assisted solution combustion method with various ratio of sorbitol/oxidizer: (a) CZA (S/N=1), (b) CZA (S/N=2) and (c) CZA (S/N=3).

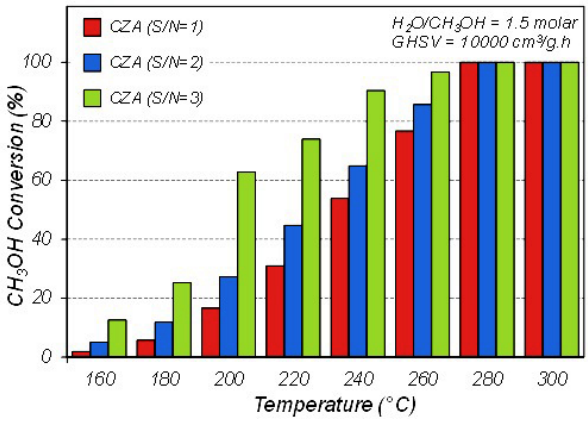

Fig. 9. Influence of the sorbitol/oxidizer ratio on methanol conversion over the microwave assisted solution combustion synthesised nanocatalysts: CZA (S/N=1), CZA (S/N=2) and CZA (S/N=3).

3.2. Catalytic performance study toward methanol steam reforming

3.2.1. Methanol conversion

The methanol conversion results shown in Figure 9 were used to investigate the role of the fuel/nitrate ratio on catalytic activity. It can be seen that enhancement of the sorbitol/oxidizer ratio led to an increase in the methanol conversion. This difference is remarkable at low temperatures where the role of nanocatalysts plays a major role in the decrease of activation energy. However, this significant performance of CZA(S/N=3) nanocatalyst was predictable due to its suitable physicochemical properties such as high surface area, homogenously small particles, narrow particle size distribution and dispersed copper particles. It is worth noting that the methanol conversion difference between CZA(S/N=3) and CZA(S/N=2) nanocatalysts is almost twice the difference between CZA(S/N=1) and CZA(S/N=2) nanocatalysts. At high temperatures, the role of nanocatalysts has been moderated due to supplying of the required heat of reaction by the external heat source. Therefore, all the nanocatalysts achieved 100% methanol conversion at 280ºC.

3.2.2. Products selectivity

Figure 10 illustrates the effect of the fuel/nitrates ratio of the fabricated nanocatalysts on SRM products selectivity. The figure demonstrates that all the samples have suitable performance for production of hydrogen as the main desired product. On the other hand, due to the utilization of produced hydrogen in fuel cell systems, the product stream must have the minimum amount of carbon monoxide as the undesired SRM product and the poison for fuel cell systems. So, it can be concluded that the CZA(S/N=3) sample produced a minimum amount of CO, which makes it more suitable for fuel cell applications. The endothermic reverse water gas shift reaction is the main side reaction for production of CO in the SRM process. The literature proved that enhancement of reaction temperature results in an increase of CO production [47, 48]. Therefore, it can be seen that for all samples the amount of CO increased as the temperature rose. However, in this case the reverse water gas shift reaction is not the only reason for production of CO. From the well-known SRM formate mechanism, we know that methanol decomposition can be taken

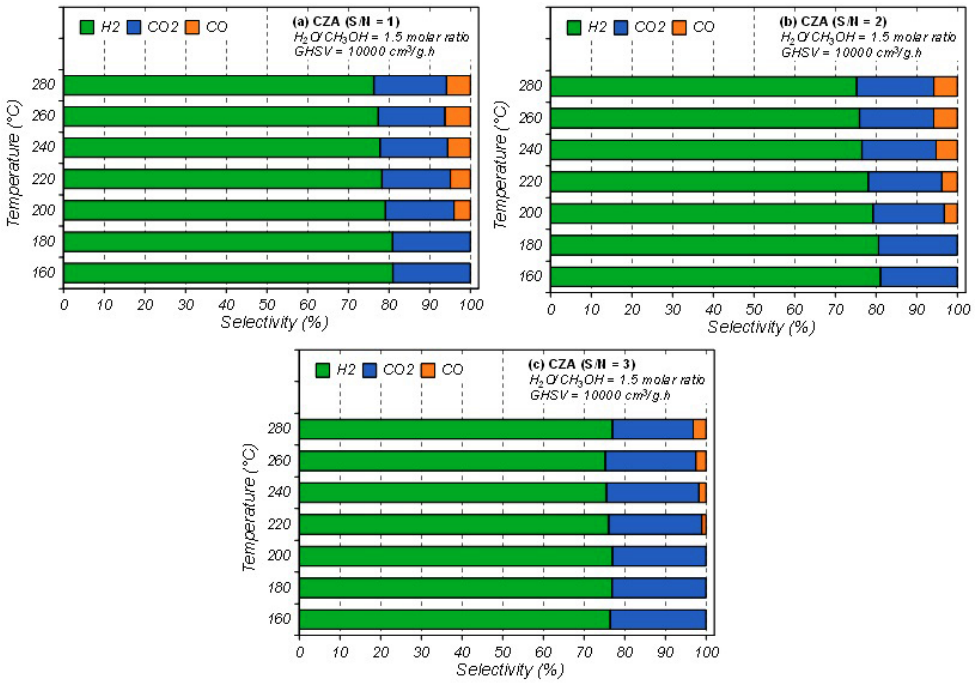

Fig. 10. Influence of the sorbitol/oxidizer ratio on products selectivity over microwave assisted solution combustion synthesised nanocatalysts: (a) CZA (S/N=1), (b) CZA (S/N=2) and (c) CZA (S/N=3).

place during SRM [49]. This means that CO can be produced via the methanol decomposition reaction. However, Karelovic and Ruiz concluded that the active copper sites of methanol decomposition and reverse water gas shift reaction are different in size [50]. The reverse water gas shift reaction can occur on smaller copper sites than the methanol decomposition reaction. So, due to the wide particle size distribution of CZA(S/N=1) and CZA(S/N=2) samples, it can be inferred that CO can be produced through both reactions. Regarding the CZA(S/N=3) nanocatalyst, because of its narrow particle size distribution the only pathway for CO production is the reverse water gas shift reaction.

3.2.3. Time on stream performance

CZA(S/N=3), which showed higher methanol conversion and low CO production, was selected to examine its stability during the SRM reaction. The time on stream performance results are shown in Figure 11. As can be seen, the methanol conversion over CZA(S/N=3) nanocatalyst did not change significantly for 1200 min. In addition, during the reaction the selectivity of products, especially CO, as the undesired product did not vary significantly. So, it can be concluded that the fabricated nanocatalysts can be an effective choice for production of hydrogen with a small amount of CO from the SRM reaction.

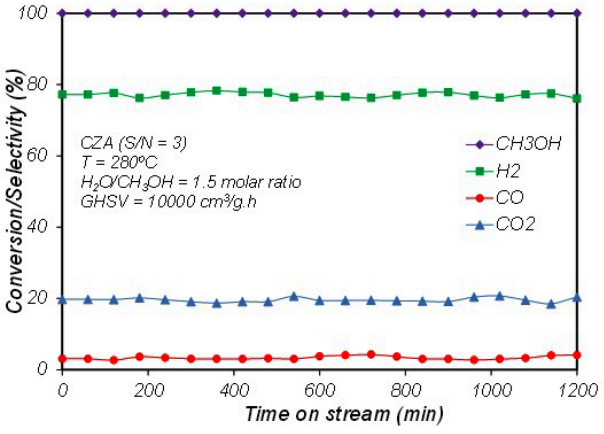

Fig. 11. Time on stream performance of CuO-ZnO-Al_2O_3 nanocatalyst synthesised with a sorbitol/oxidizer ratio of 3: CZA (S/N=3).

4. Conclusions

The characteristic analyses of the synthesized nanocatalysts demonstrated that increasing the sorbitol/nitrates ratio decreased the particle size, and consequently increased the specific surface area. Also, higher amount of fuel for preparation of nanocatalysts in the SCS method decreased the crystallinity of CuO and ZnO crystals, but enhanced their dispersion. Therefore, the CZA(S/N=3) sample which showed better physicochemical properties reached higher methanol conversion and hydrogen selectivity.

Acknowledgements

The authors gratefully acknowledge Sahand University of Technology for financial support of the research as well as the Iran Nanotechnology Initiative Council for complementary financial support.

5. References

[1] McLarty, D., Brouwer, J., and Ainscough, C., "Economic analysis of fuel cell installations at commercial buildings including regional pricing and complementary technologies", Energy and Buildings, 2016, 113: 112.

[2] Wu, H.-W., "A review of recent development: Transport and performance modeling of PEM fuel cells", Applied Energy, 2016, 165: 81.

[3] Kim, J. and Kim, T., "Compact PEM fuel cell system combined with all-in-one hydrogen generator using chemical hydride as a hydrogen source", Applied Energy, 2015, 160: 945.

[4] Kim, D.H., Kim, S.H., and Byun, J.Y., "A microreactor with metallic catalyst support for hydrogen production by partial oxidation of dimethyl ether", Chemical Engineering Journal, 2015, 280: 468.

[5] Takeishi, K. and Akaike, Y., "Hydrogen production by dimethyl ether steam reforming over copper alumina catalysts prepared using the sol-gel method", Applied Catalysis A: General, 2016, 510: 20.

[6] Carvalho, F.L.S., Asencios, Y.J.O., Bellido, J.D.A., and Assaf, E.M., "Bio-ethanol steam reforming for hydrogen production over Co_3O_4/CeO_2 catalysts synthesized by one-step polymerization method", Fuel Processing Technology, 2016, 142: 182.

[7] Ma, H., Zeng, L., Tian, H., Li, D., Wang, X., Li, X., and Gong, J., "Efficient hydrogen production from ethanol steam reforming over La-modified ordered mesoporous Ni-based catalysts", Applied Catalysis B: Environmental, 2016, 181: 321.

[8] Matsumura, Y., "Durable Cu composite catalyst for hydrogen production by high temperature methanol steam reforming", Journal of Power Sources, 2014, 272: 961.

[9] Mironova, E.Y., Lytkina, A.A., Ermilova, M.M., Efimov, M.N., Zemtsov, L.M., Orekhova, N.V., Karpacheva, G.P., Bondarenko, G.N., Muraviev, D.N., and Yaroslavtsev, A.B., "Ethanol and methanol steam reforming on transition metal catalysts supported on detonation synthesis nanodiamonds for hydrogen production", International Journal of Hydrogen Energy, 2015, 40: 3557.

[10] Shokrani, R., Haghighi, M., Jodeiri, N., Ajamein, H., and Abdollahifar, M., "Fuel cell grade hydrogen production via methanol steam reforming over $CuO/ZnO/Al_2O_3$ nanocatalyst with various oxide ratios synthesized via urea-nitrates combustion method", International Journal of Hydrogen Energy, 2014, 39: 13141.

[11] Baneshi, J., Haghighi, M., Jodeiri, N., Abdollahifar, M., and Ajamein, H., "Homogeneous precipitation synthesis of $CuO-ZrO_2-CeO_2-Al_2O_3$ nanocatalyst used in hydrogen production via methanol steam reforming for fuel cell applications", Energy Conversion and Management, 2014, 87: 928.

[12] Chen, W.-H. and Lin, B.-J., "Hydrogen production and thermal behavior of methanol autothermal reforming and steam reforming triggered by microwave heating",

International Journal of Hydrogen Energy, 2013, 38: 9973.

[13] Katiyar, N., Kumar, S., and Kumar, S., "Comparative thermodynamic analysis of adsorption, membrane and adsorption-membrane hybrid reactor systems for methanol steam reforming", International Journal of Hydrogen Energy, 2013, 38: 1363.

[14] Matsumura, Y., "Stabilization of Cu/ZnO/ZrO_2 catalyst for methanol steam reforming to hydrogen by coprecipitation on zirconia support", Journal of Power Sources, 2013, 238: 109.

[15] Zhang, L., Pan, L., Ni, C., Sun, T., Zhao, S., Wang, S., Wang, A., and Hu, Y., "CeO2-ZrO_2-promoted CuO/ZnO catalyst for methanol steam reforming", International Journal of Hydrogen Energy, 2013, 38: 4397.

[16] Das, D., Llorca, J., Dominguez, M., Colussi, S., Trovarelli, A., and Gayen, A., "Methanol steam reforming behavior of copper impregnated over CeO_2-ZrO_2 derived from a surfactant assisted coprecipitation route", International Journal of Hydrogen Energy, 2015, 40: 10463.

[17] Zhang, L., Pan, L.-w., Ni, C.-j., Sun, T.-j., Wang, S.-d., Hu, Y.-k., Wang, A.-j., and Zhao, S.-s., "Effects of precipitation aging time on the performance of CuO/ZnO/CeO_2-ZrO_2 for methanol steam reforming", Journal of Fuel Chemistry and Technology, 2013, 41: 883.

[18] Behrens, M., "Coprecipitation: An excellent tool for the synthesis of supported metal catalysts - From the understanding of the well known recipes to new materials", Catalysis Today, 2015, 246: 46.

[19] Aruna, S.T. and Mukasyan, A.S., "Combustion synthesis and nanomaterials", Current Opinion in Solid State and Materials Science, 2008, 12: 44.

[20] Mukasyan, A.S., Rogachev, A.S., and Aruna, S.T., "Combustion synthesis in nanostructured reactive systems", Advanced Powder Technology, 2015, 26: 954.

[21] González-Cortés, S.L. and Imbert, F.E., "Fundamentals, properties and applications of solid catalysts prepared by solution combustion synthesis (SCS)", Applied Catalysis A: General, 2013, 452: 117.

[22] Liu, G., Li, J., and Chen, K., "Combustion synthesis of refractory and hard materials: A review", International Journal of Refractory Metals and Hard Materials, 2013, 39: 90.

[23] Baneshi, J., Haghighi, M., Jodeiri, N., Abdollahifar, M., and Ajamein, H., "Urea-nitrate combustion synthesis of ZrO_2 and CeO_2 doped CuO/Al_2O_3 nanocatalyst used in steam reforming of biomethanol for hydrogen production", Ceramics International, 2014, 40: 14177.

[24] Srinatha, N., Dinesh Kumar, V., Nair, K.G.M., and Angadi, B., "The effect of fuel and fuel-oxidizer combinations on ZnO nanoparticles synthesized by solution combustion technique", Advanced Powder Technology, 2015, 26: 1355.

[25] Tarragó, D.P., Malfatti, C.d.F., and de Sousa, V.C., "Influence of fuel on morphology of LSM powders obtained by solution combustion synthesis", Powder Technology, 2015, 269: 481.

[26] Esmaeili, E., Khodadadi, A., and Mortazavi, Y., "Microwave-induced combustion process variables for MgO nanoparticle synthesis using polyethylene glycol and sorbitol", Journal of the European Ceramic Society, 2009, 29: 1061.

[27] Gao, Y., Meng, F., Ji, K., Song, Y., and Li, Z., "Slurry phase methanation of carbon monoxide over nanosized Ni-Al_2O_3 catalysts prepared by microwave-assisted solution combustion", Applied Catalysis A: General, 2016, 510: 74.

[28] Li, F.-t., Zhao, Y., Liu, Y., Hao, Y.-j., Liu, R.-h., and Zhao, D.-s., "Solution combustion synthesis and visible light-induced photocatalytic activity of mixed amorphous and crystalline $MgAl_2O_4$ nanopowders", Chemical Engineering Journal, 2011, 173: 750.

[29] Nassar, M.Y., Ahmed, I.S., and Samir, I., "A novel

synthetic route for magnesium aluminate ($MgAl_2O_4$) nanoparticles using sol-gel auto combustion method and their photocatalytic properties", Spectrochimica Acta Part A: Molecular and Biomolecular Spectroscopy, 2014, 131: 329.

[30] Ruiz-Gómez, M.A., Gómez-Solís, C., Zarazúa-Morín, M.E., Torres-Martínez, L.M., Juárez-Ramírez, I., Sánchez-Martínez, D., and Figueroa-Torres, M.Z., "Innovative solvo-combustion route for the rapid synthesis of MoO_3 and Sm_2O_3 materials", Ceramics International, 2014, 40: 1893.

[31] Scherrer, P., "Bestimmung der Grösse und der inneren Struktur von Kolloidteilchen mittels Röntgenstrahlen", Nachrichten von der Gesellschaft der Wissenschaften zu Gottingen, 1918, 26: 98.

[32] Allahyari, S., Haghighi, M., Ebadi, A., and Qavam Saeedi, H., "Direct synthesis of dimethyl ether as a green fuel from syngas over nanostructured CuO-ZnO-Al_2O_3/HZSM-5 catalyst: Influence of irradiation time on nanocatalyst properties and catalytic performance", Journal of Power Sources, 2014, 272: 929.

[33] Allahyari, S., Haghighi, M., and Ebadi, A., "Direct synthesis of DME over nanostructured CuO-ZnO-Al_2O_3/HZSM-5 catalyst washcoated on high pressure microreactor: Effect of catalyst loading and process condition on reactor performance", Chemical Engineering Journal, 2015, 262: 1175.

[34] Abramoff, M.D., Magalhaes, P.J., and Ram, S.J., "Image Processing with ImageJ", Biophotonics International, 2004, 11: 36−42.

[35] Estifaee, P., Haghighi, M., Mohammadi, N., and Rahmani, F., "CO oxidation over sonochemically synthesized Pd-Cu/Al_2O_3 nanocatalyst used in hydrogen purification: Effect of Pd loading and ultrasound irradiation time", Ultrasonics Sonochemistry, 2014, 21: 1155.

[36] Khoshbin, R., Haghighi, M., and Asgari, N., "Direct synthesis of dimethyl ether on the admixed nanocatalysts of CuO-ZnO-Al_2O_3 and HNO_3-modified clinoptilolite at high pressures: Surface properties and catalytic performance", Materials Research Bulletin, 2013, 48: 767.

[37] Allahyari, S., Haghighi, M., Ebadi, A., and Hosseinzadeh, S., "Effect of irradiation power and time on ultrasound assisted co-precipitation of nanostructured CuO-ZnO-Al_2O_3 over HZSM-5 used for direct conversion of syngas to DME as a green fuel", Energy Conversion and Management, 2014, 83: 212.

[38] Allahyari, S., Haghighi, M., and Ebadi, A., "Direct conversion of syngas to DME as a green fuel in a high pressure microreactor: Influence of slurry solid content on characteristics and reactivity of washcoated CuO-ZnO-Al_2O_3/HZSM-5 nanocatalyst", Chemical Engineering and Processing: Process Intensification, 2014, 86: 53.

[39] Charghand, M., Haghighi, M., and Aghamohammadi, S., "The Beneficial Use of Ultrasound in Synthesis of Nanostructured Ce-Doped SAPO-34 Used in Methanol Conversion to Light Olefins", Ultrasonics Sonochemistry, 2014, 21: 1827.

[40] Sajjadi, S.M., Haghighi, M., and Rahmani, F., "Dry Reforming of Greenhouse Gases CH_4/CO_2 over MgO-Promoted Ni-Co/Al_2O_3-ZrO_2 Nanocatalyst: Effect of MgO Addition via Sol-Gel Method on Catalytic Properties and Hydrogen Yield", J Sol-Gel Sci Technol, 2014, 70: 111.

[41] Khoshbin, R. and Haghighi, M., "Urea-Nitrate Combustion Synthesis and Physicochemical Characterization of CuO-ZnO-Al_2O_3 Nanoparticles over HZSM-5", Chinese Journal of Inorganic Chemistry, 2012, 28: 1967.

[42] Aghaei, E. and Haghighi, M., "Effect of Crystallization Time on Properties and Catalytic Performance of Nanostructured SAPO-34 Molecular Sieve Synthesized at High Temperatures for Conversion of Methanol to Light Olefins", Powder Technology, 2015, 269: 358.

[43] Asgari, N., Haghighi, M., and Shafiei, S., "Synthesis and Physicochemical Characterization of Nanostructured CeO_2/Clinoptilolite for Catalytic Total Oxidation of

Xylene at Low Temperature", Environmental Progress and Sustainable Energy, 2013, 32: 587.

[44] Saedy, S., Haghighi, M., and Amirkhosrow, M., "Hydrothermal synthesis and physicochemical characterization of CuO/ZnO/Al_2O_3 nanopowder. Part I: Effect of crystallization time", Particuology, 2012, 10: 729.

[45] Rahmani, F., Haghighi, M., Vafaeian, Y., and Estifaee, P., "Hydrogen Production via CO_2 Reforming of Methane over ZrO_2-Doped Ni/ZSM-5 Nanostructured Catalyst Prepared by Ultrasound Assisted Sequential Impregnation Method", Journal of Power Sources, 2014, 272: 816.

[46] Sharifi, M., Haghighi, M., and Abdollahifar, M., "Hydrogen Production via Reforming of Biogas over Nanostructured Ni/Y Catalyst: Effect of Ultrasound Irradiation and Ni-Content on Catalyst Properties and Performance", Materials Research Bulletin, 2014, 60: 328.

[47] Wang, C., Liu, C., Fu, W., Bao, Z., Zhang, J., Ding, W., Chou, K., and Li, Q., "The water-gas shift reaction for hydrogen production from coke oven gas over Cu/ZnO/Al_2O_3 catalyst", Catalysis Today, 2016, 263: 46.

[48] Wilkinson, S.K., van de Water, L.G.A., Miller, B., Simmons, M.J.H., Stitt, E.H., and Watson, M.J., "Understanding the generation of methanol synthesis and water gas shift activity over copper-based catalysts – A spatially resolved experimental kinetic study using steady and non-steady state operation under $CO/CO_2/H_2$ feeds", Journal of Catalysis, 2016, 337: 208.

[49] Lin, S., Johnson, R.S., Smith, G.K., Xie, D., and Guo, H., "Pathways for methanol steam reforming involvingadsorbed formaldehyde and hydroxyl intermediates on Cu (111): density functional theory studies", Physical Chemistry Chemical Physics, 2011, 13: 9622.

[50] Karelovic, A. and Ruiz, P., "The role of copper particle size in low pressure methanol synthesis via CO_2 hydrogenation over Cu/ZnO catalysts", Catalysis Science & Technology, 2015, 5: 869.